

UCLA

UCLA Previously Published Works

Title

Construction and characterization of a frequency-controlled, picometer-resolution, displacement encoder-actuator

Permalink

<https://escholarship.org/uc/item/0ws69349>

Journal

Review of Scientific Instruments, 87(5)

Authors

Koulakis, John Pandelis
Stein, Michael
Holzcer, Karoly

Publication Date

2016-05-23

Data Availability

The data associated with this publication are within the manuscript.

Peer reviewed

Construction and Characterization of a Frequency-Controlled, Picometer-Resolution, Displacement Encoder-Actuator

John P. Koulakis,¹ Michael Stein, and Károly Holczer^{1, a)}

Department of Physics and Astronomy, University of California Los Angeles, Los Angeles, California 90095, USA

We have constructed an actuator/encoder whose generated displacement is controlled through the resonance frequency of a microwave cavity. A compact, 10- μm -range, digitally-controlled actuator executing frequency-coded displacement with picometer resolution is described. We consider this approach particularly suitable for metrologic-precision scanning probe microscopy.

The easy mechanical tunability of microwave cavities has been exploited in applications ranging from broadband, mechanically-tuned microwave oscillators and filters to gravitational wave detection¹ thanks to the ever growing variety of resonator structures and frequency locking schemes. High sensitivity transducers based on microwave cavities² have been reported as well. In this paper we describe a microwave cavity and controller that function as a displacement actuator system designed specifically for Scanning Probe Microscopy (SPM) applications.

Positioning in scanning probe microscopy represents a particular challenge due to the enormous dynamic range ($> 10^7$) of the piezo-electric actuators used. While lateral (x-y) scan ranges of 3-100 μm are common, acquiring images with distance scales that can be trusted at the sub-angstrom (< 100 pm) level remains a challenge. Reducing both 1) positioning noise and 2) scanner drift over the timescale of image acquisition to required levels is achieved reproducibly at low temperature³, and inconsistently in less-controlled conditions. A search for a reasonable way to build a metrologic instrument capable of making surface atomic-reconstruction measurements with precision comparable to that of crystallographic data, is the motivation of this work. The minimum requirement to achieve that, is an active-feedback-controlled distance encoder with ~ 10 μm working range and > 1 kHz bandwidth response, combined with picometer-scale accuracy, linearity, and long-term stability. We demonstrate a device and control system that meets all these requirements in a smaller, simpler configuration than other methods⁴ under development. In addition, it is intrinsically traceable; relying on frequency standards and the speed of light to set the distance scale.

Our frequency-controlled displacement encoder-actuator is a microwave cavity whose length is actively controlled to keep its resonant frequency matched to the setpoint. The resonant frequencies, f_n , of the TEM_{00n} modes of a coaxial resonator are related to its length L , through $f_n = nc/2L$. The frequency's independence of all other dimensions makes these modes the most suitable for our purpose, in spite of the fact that they are

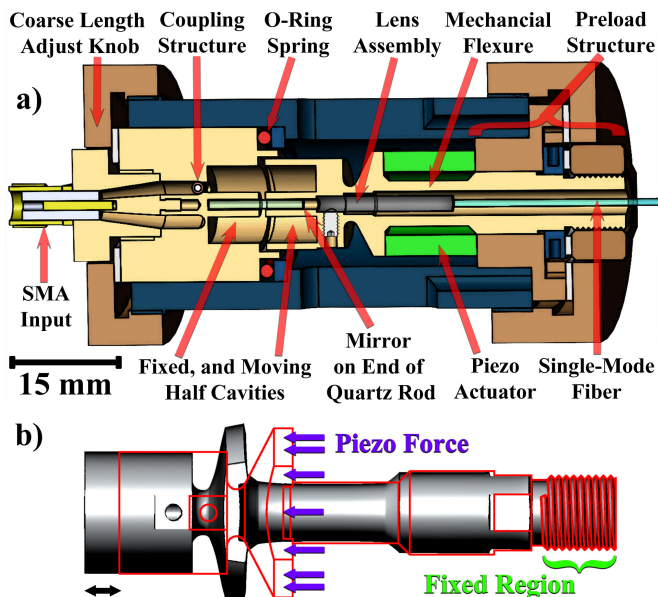


FIG. 1. a) Cross section of the displacement encoder assembly, which incorporates the coupling structure, the resonant cavity, a mechanical flexure, and an optical interferometer along the axis to independently measure the relative displacement of the cavity halves. The moving half-cavity is machined into the end of an aluminum tube that is stretched by a concentric stacked-piezo tube to the deformed shape shown in b). The exaggerated deformation (shaded model) is to be compared to the zero-strain shape indicated by the red wire-frame model.

relatively low quality factor (Q) modes. To keep it compact, we choose to build a 15 mm length cavity working at its lowest frequency ($n=1$) mode, at 10 GHz. The practical realization required building a variable-length cavity, with a coupling that is minimally perturbed by the length change, as well as a sub-millihertz-resolution microwave control system with 10^{-12} stability.

Figure 1a shows a cross section of the constructed mechanical assembly. The adjustable length is realized by cutting the cavity along a plane perpendicular to the axis and equidistant from the ends. There is no current flowing in the walls there and therefore the Q and the resonant frequency of the cavity are unaffected by a small gap. The left half-cavity is tied to the end of the external tube housing the device - indicated as the “Fixed”

^{a)}holczer@physics.ucla.edu

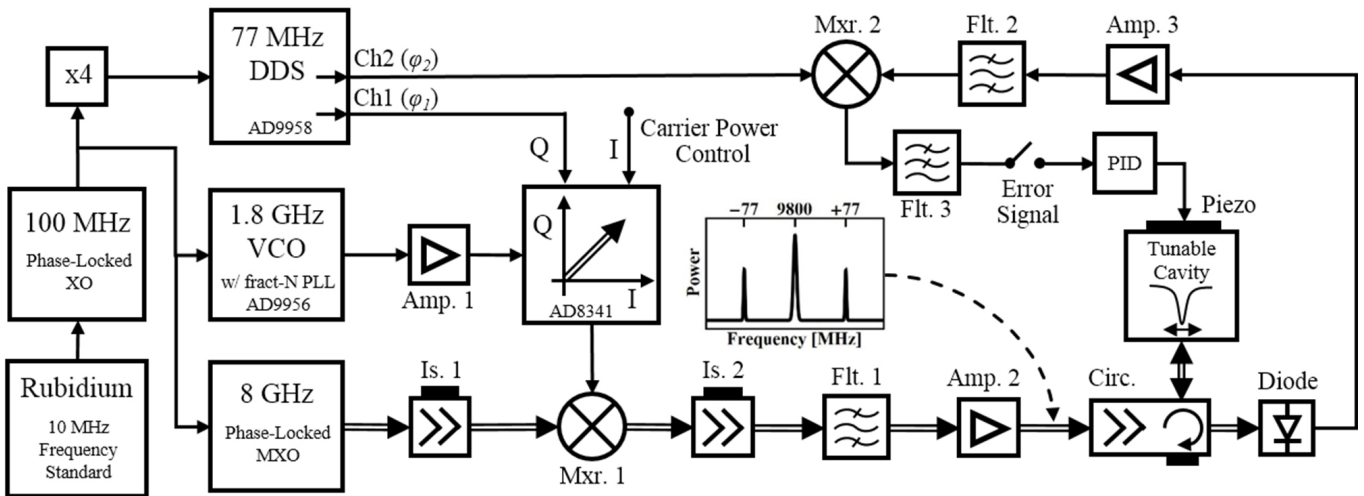


FIG. 2. The cavity resonance frequency is measured with a microwave version of a Pound-Drever-Hall lock, which generates a signal proportional to the difference between the source and cavity frequencies. This is used as an error signal in a feedback loop to lock the cavity to the source, transferring the stability of the rubidium frequency reference, and the precise, digital tunability of the microwave source, to the cavity length. Double-lined arrows indicate the path of high frequency (≥ 8 GHz) signals, while single-lined arrows indicate low frequency signals. The inset indicates the spectrum of the generated signal: a carrier and two phase-modulation-like sidebands. Amp: Amplifier, Is: Isolator, Mxr: Mixer, Flt: Filter, Circ: Circulator.

Half in the figure - setting the coarse length of the cavity. The holder of the “Moving” Half - attached to the right end of the housing tube - is variable length. A stacked-piezo tube (Piezomechanic HPSt 150/14-10/12), kept under compressive load throughout its stroke, allows elastic elongation of the concentric aluminum tube over a 10 μm range (figure 1b). The shape of the variable-length holder is designed to minimize any bending of the cavity walls. By applying a layer of damping material (spray-on rubber sealant - not shown) around the flexure tube, the stability of the feedback loop could be extended from about 2 kHz to 8 kHz. Both half-cavity pieces were fabricated out of aluminum 7075 and subsequently gold plated, resulting in a loaded Q of 1280.

While the 15 mm cavity length is set by the choice of the 10 GHz working frequency, the 3.5 mm and 11 mm inner and outer diameter were chosen as a compromise between quality factor, coupling dynamic range, and size constraints. An oversized coaxial waveguide (whose inner diameter matches that of the cavity’s inner conductor), ending with a half-toroidal curved wall, brings the microwaves close to the fixed half-cavity end wall, and a taper element allows connecting it to a standard SMA connector. Coupling is done with an iris (small hole) on the cavity/waveguide wall, which is partially blocked by a floating copper pill held in place by a dielectric (PEEK) screw. Moving the pill in front of the iris allows precise control of the coupling, over a range $0.8 < \beta < 1.2$, where the coupling parameter $\beta = (1 \pm |S|)/(1 \mp |S|)$, and S is the scattering parameter on resonance; the top (bottom) sign is chosen for over- (under-) coupled cases⁵. We have found that a return loss greater than 50 dB optimizes the signal-to-noise ratio in our system, necessitating a

smoothly-working adjustable coupling.

An error signal for closed-loop control is generated by comparing the cavity resonance frequency to that generated by a home-built microwave source, whose block diagram is shown in figure 2. We have implemented a microwave version of what is commonly known in optics as a Pound-Drever-Hall (PDH) lock^{1,6}. Closing the loop drives the piezo-actuator to match the cavity resonance frequency to that of the microwave signal. The cavity frequency inherits the stability and digital tunability of the source, stable to ~ 10 mHz, and adjustable in the range of 9810 ± 15 MHz, with better than millihertz precision.

The frequency modulated 9.8 GHz signal is generated in multiple steps. All signal sources are phase-locked directly or indirectly to a rubidium frequency reference (SRS PRS10), ensuring 2×10^{-12} stability over 100 s. The fine frequency control and modulation is implemented at 1.8 GHz, and then converted up to 9.8 GHz using an 8 GHz low phase-noise source (Wenzel multiplied crystal oscillator (MXO)). A 1810 ± 15 MHz VCO (ZCommunications ZRO1820A1LF) is controlled via a fractional-N phase-lock-loop (PLL) that internally includes a direct digital synthesizer (DDS) chip with a 48-bit frequency tuning word (Analog Devices AD9956). The reference for the PLL is a 100 MHz crystal oscillator (Wenzel SC-cut XO) with low close-in phase noise. This configuration provides digital frequency control with ~ 11 μHz resolution. The VCO output is taken to a vector (IQ) modulator (Analog Devices AD8341), which amplitude modulates ($\pm 100\%$, as in double-sideband suppressed-carrier transmission) the Q component at a frequency of 77 MHz. The modulation frequency, generated by channel 1 of a two-channel DDS board (Analog

Devices AD9958), is chosen to be much higher than the cavity half-width (3.8 MHz) for reasons discussed below. The I component is not modulated, but optionally attenuated by setting the DC voltage on the I baseband input. The resulting output of the vector modulator is a carrier at 1.8 GHz, and two sidebands at ± 77 MHz. This is converted up to 9.8 GHz (figure 2 inset), amplified to 12 dBm carrier and -12 dBm sideband power, and directed to the coarsely frequency-matched cavity through a circulator.

Since the carrier frequency is close to the cavity resonance, its reflection is phase shifted proportionally with the frequency difference, undergoing a π phase change over the cavity width. The sidebands, chosen to be far from the cavity, are reflected with constant phase, and serve as a reference for measuring the phase-shift of the carrier. After detection with a biased Schottky diode (Herotek DDS118), the beating of the sidebands with the carrier is selectively detected with the help of a mixer and the properly-phased reference, provided by the channel 2 output of the DDS board, to generate the microwave PDH error signal. Calibration of the error signal is achieved by measuring its response to a known change in the source frequency. It is optionally fed-back to the cavity piezo through a PID amplifier to lock the cavity to the source. An Asylum Research MFP3D controller conveniently provides several analog-to-digital and digital-to-analog converters, a -10 to +150 V high voltage amplifier, and digital PID loop needed to run and monitor the system. Software to set power levels, frequencies, and/or phase of the various signal generators was written in Wavemetrics IGOR Pro.

To independently measure the cavity motion, an optical interferometer was added along its axis (figure 1a). A single-mode-fiber-coupled 1310 nm laser diode was used as a light source. Light was brought through a fiber-coupled circulator to a lens assembly consisting of a gradient index lens and a 3 mm radius plano-concave lens affixed to the moving half-cavity. The 3 mm working distance of the lens assembly assures that light rays stepping to air from glass are perpendicular to the concave surface, which is not anti-reflection coated to provide a proper reference surface to a flat mirror placed at the beam waist. An aluminum-coated end of a polished quartz rod is held by the fixed half-cavity at the beam waist. The lens collects the back-reflected light, as well as the $\sim 4\%$ reflected off the concave glass-air interface, and couples them back into the single-mode fiber. They are directed by the circulator to a photodiode, and the observed interference signal reflects the distance change between the concave lens surface and the end of the quartz rod, allowing observation of the relative motion of the microwave cavity halves.

Our system is used as an actuator in closed-loop active feedback mode, controlling the motion through setting the frequency value. A change of the source frequency in open-loop produces a step in the error signal (“Open-Loop” curve in figure 3b), whose 9 μ s settling

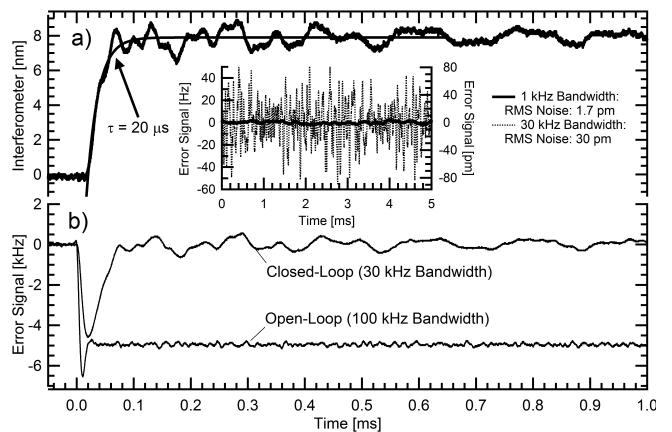


FIG. 3. A 5 kHz change in the source frequency (setpoint) of our encoder-actuator produces an 8 nm displacement of the microwave cavity halves, as seen in the interferometer signal a). For this measurement, the cavity frequency was set so that the interferometer was sensitive to small displacements (at a zero crossing of figure 5). The mechanically-limited response time has a time-constant of 20 μ s. b) The open- and closed-loop microwave PDH error signal. Ringing of 2 nm amplitude is observed on the closed-loop error signal and interferometer signal, and indicates that further damping might be beneficial. Inset displays the noise level on the open-loop error signal, equal to 1.1 Hz or 1.7 pm RMS in a 1 kHz bandwidth.

time is characteristic of our microwave source. In closed-loop, the error signal drives the piezo to adjust the cavity length. The resulting motion is captured by the interferometer (figure 3a) and brings the error signal back to zero (“Closed-Loop” in figure 3b). The exponential settling time of the mechanical response to a 5 kHz (8 nm) step in the setpoint⁷ was 20 μ s (8 kHz mechanical bandwidth). While adding payload, i.e. the mass of a sample holder, will reduce the bandwidth, we estimate that a scanner using this actuator would be able to collect up to 3 full-scale, 1024×1024 images per minute. The inset displays the noise level on the open-loop error signal, which can be reduced to 1.7 pm RMS if 1 kHz bandwidth is sufficient.

The precision of the system is determined by the quality of the microwave sources used. The frequency analysis of the microwave PDH error signal is shown both for closed- and open-loop operation in figure 4. The open-loop noise spectral density curve shows a minimum of 60 fm $\text{Hz}^{-1/2}$ around 500 Hz as the low frequency noise is dominated by the cavity frequency noise; we have made no particular effort to isolate vibrational and acoustical noise from the cavity. As the mechanical noise diminishes at higher frequencies, the frequency difference noise starts to get dominated by the phase noise of the microwave signal sources. Turning on the feedback loop actively compensates the vibration and acoustic noise, but also converts phase noise to length fluctuations within the loop bandwidth. Above the loop bandwidth (1 kHz in the figure), the closed loop signal practically matches

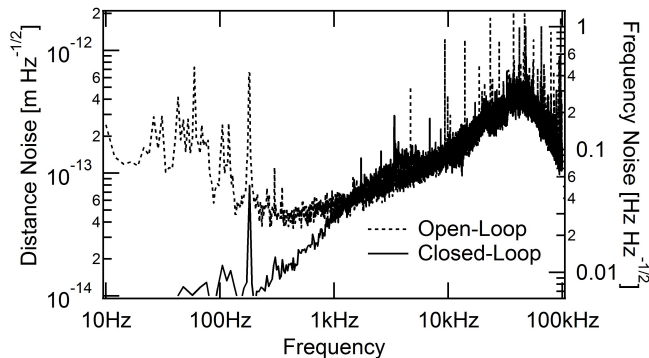


FIG. 4. The noise spectral density of the open and closed loop PDH error signal. The open-loop, low-frequency noise is due to cavity vibration and drift. Closing the loop stabilizes the cavity, suppressing drift and vibration within the loop bandwidth.

the open loop signal. From a noise and stability point-of-view, the optimal bandwidth is where the diminishing (in frequency) mechanical noise intersects the increasing frequency noise of the source. In practice however, the bandwidth is chosen as a compromise between RMS noise and settling time. Limiting the feedback bandwidth to 1 kHz, and taking the distance noise to be $60 \text{ fm Hz}^{-1/2}$ everywhere in this range allows us to claim less than 2 pm RMS noise in a 1 kHz bandwidth.

We note that the precision of any other Automatic Frequency Control (AFC) method⁸ implemented instead of our microwave PDH scheme would also be ultimately limited by the phase stability of the source. The realized microwave PDH system advantage is a fast response time allowing us to explore the limitations of our mechanical design.

Obviously, the fiber interferometer built into the middle of the cavity was never meant to verify the precision claimed, but it was useful to characterize the overall system behavior, such as scan range, bandwidth, piezo-hysteresis, and linearity. Figure 5 illustrates the interferometer signal, showing subsequent fringes obtained during a full range scan. We verified a $12 \text{ }\mu\text{m}$ range by counting fringes; this could be extended somewhat with a different choice of piezo and high-voltage amplifier, but a different mechanical design would be necessary beyond that. The voltage applied to the piezo is displayed in the inset, demonstrating its hysteresis.

To obtain the range within which the ideal frequency relation $f = c/2L$ is obeyed, we fit parabolas to locate successive minima or maxima in the interferometer signal (blue and green curves in figure 5) and extracted the frequency difference corresponding to the $\lambda/2$ (655 nm) periodicity with $\pm 0.5\%$ ($\pm 3 \text{ nm}$) precision, as a function of frequency, reproducibly. We averaged the fringe spacing from an equal number of forward and backward scans (10 each) to compensate for drifts. This precision would not allow us to detect any deviations from the ideal relation $f = c/2L$ if the gap between the cavity halves is

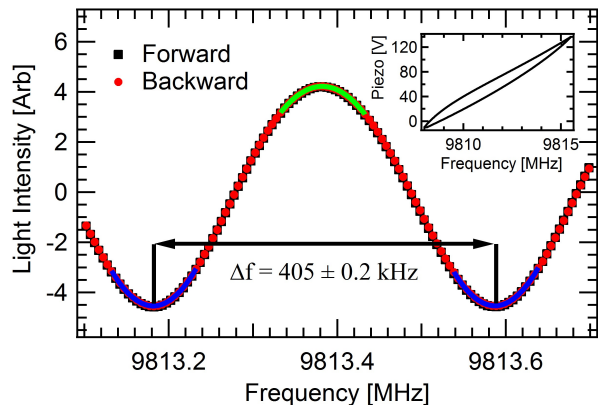


FIG. 5. (Color online) The $\lambda/2$ periodicity of the interferometer signal as the cavity frequency is scanned in closed-loop is used to verify that the relationship $\Delta L = -c\Delta f/2f^2$ is obeyed in a limited range. We verified a 5% deviation at a $120 \text{ }\mu\text{m}$ gap between the cavity halves. The hysteresis of the piezo during a full, $12 \text{ }\mu\text{m}$ range scan is displayed in the inset.

less than $10 \text{ }\mu\text{m}$. Our differential measurement would be indistinguishable from $\Delta L = -c\Delta f/2f^2$. We have simulated the cavity frequency as a function of the gap width⁹ in Ansys HFSS. The quadratic correction results in a 1% and 5% deviation in the linearized frequency-distance relationship at 45 and $120 \text{ }\mu\text{m}$ respectively. The 5% deviation with a $120 \text{ }\mu\text{m}$ gap was sufficiently significant to verify with our interferometer within the experimental error (figure 5). The back extrapolation of the values confirms that less than 0.1% deviation from the ideal slope is expected when the gap is reduced to the 0-10 μm range. Since the $\pm 0.5\%$ irreproducibility - due to small changes in the cavity alignment when the assembly is rebuilt and/or the cavity length is coarsely adjusted (knob in figure 1a) - is larger, we claim that as our absolute uncertainty. If the coarse mechanics are not adjusted, the measurement is reproducible at the 10^{-4} level.

It is instructive to consider challenges encountered with atomic-resolution metrology on the Molecular Measuring Machine (M^3) at NIST^{10,11}. M^3 's ambitious goal of several 10s of millimeter range led to the choice of polarization-encoded heterodyne interferometers to control the x and y motion. Their noise level is a few 100 pm in a relatively low bandwidth - prohibiting atomic-scale, closed-loop imaging. Further, over the 80 nm fringe period, there is a 2 nm non-linearity, resulting in as much as an 8% deviation of measured lattice parameters (in materials with large lattice constants) from bulk crystal x-ray diffraction measurements. Of course, open-loop imaging is capable of achieving atomic-resolution images, but then piezo creep and non-linearities result in images with an apparently varying lattice constant and uncertain scale. With the picometer-resolution, kilohertz-bandwidth, displacement encoder we present, closed-loop atomic-scale imaging is possible within a $10 \text{ }\mu\text{m}$ range - which is already excessive if the goal is to study atomic

reconstruction at material surfaces. The non-linearity of our device would appear as variation of the lattice constant between one side of the image and the other, of less than 1 part in 10^4 . Consequently, atomic scale distances as well as periodicities (revealed by Fourier transformation of data collected over the full range) would be determined with better than 1% precision, comparable to that of lattice parameters obtained by bulk crystallography.

Incorporating such an encoder into the positioning stage of an SPM would require two encoders to operate in perpendicular directions with minimal cross-talk. This demands a mechanical scheme that decouples the motion of one cavity from the other, a direction of research we are pursuing. Our active stabilization scheme matches the electrical length of the microwave cavity to the wavelength of the source. To capitalize on the stability offered by frequency standards, stringent environmental control is needed to eliminate variations of the dielectric constant of the gas within the cavity¹², the cavity wall resistivity¹³, just as well as the rest of the scanner to limit drift of all mechanical parts involved. For a 15 mm cavity placed in vacuum, the effective “thermal coefficient” of the encoder is expected to be $1.7 \times 10^{-7} \text{ K}^{-1}$ over the cavity length, almost an order of magnitude smaller than that of Invar.

We have demonstrated that compact, coaxial microwave cavities make excellent displacement measurement tools, capable of picometer precision. The described device has a range of 10 μm , limited by the chosen piezo-actuator, and a noise floor of 60 fm $\text{Hz}^{-1/2}$, limited by the quality of the signal generators. As is, the system accuracy is 0.5% of the measured displacement, without external calibration. With finer mechanics, the system is capable of better than 0.1% accuracy, although for ranges larger than 10s of micrometer, a non-linear correction will be needed to account for the larger gap. Incorporating displacement encoders using these principles into SPM would go a considerable way towards realization of a metrological SPM capable of surface atomic-reconstruction measurements.

ACKNOWLEDGMENTS

We thank Emil Kirilov for valuable discussions, Asylum Research for electronics and technical support,

and the UCLA physics machine shop for fabricating the intricate pieces in this work.

- ¹A. G. Mann and D. G. Blair, *Journal of Physics D: Applied Physics* **16**, 105 (1983).
- ²D. G. Blair, E. N. Ivanov, and H. Peng, *Journal of Physics D: Applied Physics* **25**, 1110 (1992); B. D. Cuthbertson, M. E. Tobar, E. N. Ivanov, and D. G. Blair, *IEEE Transactions on Ultrasonics, Ferroelectrics, and Frequency Control* **45**, 1303 (1998).
- ³J.-X. Zhu, K. McElroy, J. Lee, T. P. Devereaux, Q. Si, J. C. Davis, and A. V. Balatsky, *Phys. Rev. Lett.* **97**, 177001 (2006); T. Hanaguri, Y. Kohsaka, J. C. Davis, C. Lupien, I. Yamada, M. Azuma, M. Takano, K. Ohishi, M. Ono, and H. Takagi, *NATURE PHYSICS* **3**, 865 (2007).
- ⁴M. Pisani, A. Yacoot, P. Balling, N. Bancone, C. Birlikseven, M. Celik, J. Fluegge, R. Hamid, P. Koechert, P. Kren, U. Kuetgens, A. Lassila, G. B. Picotto, E. Sahin, J. Seppa, M. Tedaldi, and C. Weichert, *Metrologia* **49**, 455 (2012).
- ⁵G. Hammer, S. Wuensch, M. Roesch, K. Ilin, E. Crocoll, and M. Siegel, *IEEE TRANSACTIONS ON APPLIED SUPERCONDUCTIVITY* **19**, 565 (2009).
- ⁶S. R. Stein and J. P. Turneaure, *Electronics Letters* **8**, 321 (1972); in *27th Annual Frequency Control Symposium* (1973) pp. 414–420; R. W. P. Drever, J. L. Hall, F. V. Kowalski, J. Hough, G. M. Ford, A. J. Munley, and H. Ward, *Applied Physics B* **31**, 97 (1983); E. D. Black, *American Journal of Physics* **69**, 79 (2001).
- ⁷This required using an analog PID (SRS SIM960) because of a 70 μs delay associated with the digital electronics. For other measurements reported, the digital PID was used, limiting the bandwidth to 1 kHz.
- ⁸R. V. Pound, *The Review of Scientific Instruments* **17**, 490 (1946).
- ⁹J. P. Koulakis, “Traceable and Precise Displacement Measurements with Microwave Cavities,” (2014), copyright ProQuest, UMI Dissertations Publishing 2014;.
- ¹⁰J. A. Kramar, R. Dixon, and N. G. Orji, *Measurement Science & Technology* **22** (2011).
- ¹¹J. A. Kramar, *Measurement Science & Technology* **16** (2005).
- ¹²It was observed that thermal and humidity fluctuations caused the largest changes in the dielectric constant of the air within the cavity sitting in atmosphere⁹.
- ¹³Drift of about 2.5 nm K^{-1} can be expected based on the thermal coefficient of resistivity for common, high-conductivity metals.